Improvement of the formulation of the dispersed phase boundary conditions for a rough wall needed in two-fluid models

Mohammed Khalij, Boris Arcen, Anne Tanière

IMPROVEMENT OF THE FORMULATION OF THE DISPERSED PHASE BOUNDARY CONDITIONS FOR A ROUGH WALL NEEDED IN TWO-FLUID MODELS

M. Khalij, B. Arcen , A. Tanière*

* LEMTA (LUMEN Group) – UMR 7563 CNRS, Université Henri Poincaré - Nancy 1
ESSTIN, 2 rue Jean Lamour, 54519 Vandoeuvre-lès-Nancy, France
e-mail: taniere@esstin.uhp-nancy.fr

ABSTRACT

The dispersed phase wall boundary conditions for gas-particle flows are investigated here taking the effects of 3-D wall roughness on frictional inelastic particle-wall collisions and taking the anisotropy of the particle velocity fluctuations into account. Particle statistics at the wall are computed by simulating a large number of particle-wall impacts for a Gaussian distribution of the incident wall normal velocity. The collisions are treated by using a 3-D irregular bouncing model and avoiding unphysical impact or reflected angles, the so-called shadow effect. The approach which allows to derive the dispersed phase boundary conditions in the case of rough wall is described. By taking the zero mass flux condition and the shadow effect into account, the second and third order particle velocity correlations at the wall can be compared to the theoretical relations obtained in the smooth case. Equivalent friction and restitution coefficients are defined, making it possible to use the same formulation of the dispersed phase boundary conditions as established in the smooth wall case. The dependence of these equivalent coefficients upon the actual collision parameters and the wall roughness is illustrated by the results of the numerical simulation.

1 INTRODUCTION

One of the approach which can be used for the numerical simulation of dispersed two-phase flows is the so-called Eulerian-Eulerian approach commonly named “the two-fluid model”. It is easier to take the presence of the wall into account by Lagrangian simulation, just by using rebound laws and introducing the effect of particle shape or wall roughness by means of a virtual wall model (Tsuji *et al.* [1], Sommerfeld [2], Sommerfeld and Huber [3]). In two-fluid models, the wall exists only through the boundary conditions needed for the solution of the differential system. In order to obtain accurate information about the influence of the wall on the behaviour of solid particles, it is important to develop a set of boundary conditions for the dispersed phase. Many works have been devoted to the study of the dispersed phase boundary conditions at the wall. Derevich and Zaichik [4] have used the kinetic equation for probability density function (PDF) of particle coordinates and velocity distribution for the particle deposition. They have obtained a solution for their model at the wall by a perturbation method function of a reflection coefficient. Swailes and Reeks [5] have also used a PDF model (Kinetic equation) for steady-state transport and deposition of particle for partially or perfectly reflection at the wall . In the last case, elastic rebounds are considered and the boundary conditions have been obtained by a spectral method. Devenish *et al.* [6] have extended this work for inelastic particle–wall collisions and for a restitution coefficients higher than 0.5. He and Simonin [8] and Sakiz and Simonin [9] have established a set of boundary conditions for the dispersed phase at a smooth wall in terms of the Coulomb parameters (coefficients of friction and restitution), using a preassigned binormal PDF for the wall normal particle velocity. Their formalism is based on the determination of PDF of the particle velocities close to the wall. Using this PDF-two-fluid method, the mean value of any variable at the wall can be expressed as a function of the mean value before collision, and relationships between the various statistical moments of the particle velocity components can be derived, provided that a deterministic rebound law is prescribed. Alipchenckov *et al.* [7] have compared the results given by a perturbation method with the results obtained by a binormal PDF method for the phase dispersed. They showed that the approach using the resolution of the PDF equation by the perturbation method is only accurate for particle rebounds slightly inelastic whereas the binormal PDF method could be applied for a large range of the restitution coefficient. Nevertheless, all these studies are valid only with a smooth wall. In a rough case, no work exists about Eulerian dispersed phase boundary conditions taking the effect of the 3-D roughness into account. The work of Zhang and Zhou [10] is limited to a 2-D roughness case simulated with the help of a virtual wall model (Sommerfeld [2]) and without taking the shadow effect into account. This physical phenomenon has been revealed by Sommerfeld and Huber [3]. According to us, to obtain a realistic simulation of the particle-wall interaction when a virtual wall model (Sommerfeld [2]) is used, some generated angles have to be eliminated since they can be unphysical. The establishment of boundary conditions incorporating the effect of wall roughness is identified as one of the objectives pursued in this paper. We propose here to introduce the effect of the 3-D roughness *via* the use of a virtual wall model based on the idea of Sommerfeld and Zivkovic [11]. No deposition phenomenon of particles was considered here. Before presenting and discussing the numerical simulation results issued from a statistical study on a large number of particle rebounds at the wall, the derivation of the dispersed phase boundary conditions for a rough wall is described. It is based on an analogy with the formalism established for a smooth

wall. Equivalent restitution and friction coefficients are introduced and their dependence on the roughness parameter is studied.

2 ROUGH WALL BOUNDARY CONDITIONS DERIVATION

2.1 Description of the proposal model

As Sakiz and Simonin [9], we consider a distribution function f for the velocity of the particles at the wall. The mean value of any function y of the velocity can be given by:

$$\langle y\,(\mathbf{u})\rangle = \frac{1}{N}\int y\,(\mathbf{u})\; f\,(\mathbf{u})\, d\,\mathbf{u} \tag{1}$$

where $N = \int f\,(\mathbf{u})\, d\,\mathbf{u}$ is the particle number density at the wall.

The fluctuation of y is defined by $y' = y - \langle y \rangle$. In order to focus on the effect of the rebounds on the wall, as Sakiz and Simonin [9], we distinguish the mean values of y for incident $\langle . \rangle^-$ and reflected particles $\langle . \rangle^+$, linked by the following relation:

$$N \langle y \rangle = N^- \langle y \rangle^- + N^+ \langle y \rangle^+ \tag{2}$$

where N^- and N^+ are the number densities of incident and reflected particles at the wall, respectively, so that $N = N^- + N^+$. Equation (2) can be written using the parameter x defined by $x = N^-/N$:

$$\langle y \rangle = x \langle y \rangle^- + (1-x)\langle y \rangle^+ \tag{3}$$

The relation (Eq. (3)), written for $y = u_Y$, shows that the parameter x must therefore satisfy the following condition in order to have a zero particle mass flux at the wall (*i.e.* $\langle u_Y \rangle = 0$):

$$x = \frac{N^-}{N} = \frac{\langle \tilde{u}_Y \rangle^+}{\langle \tilde{u}_Y \rangle^+ - \langle u_Y \rangle^-} \tag{4}$$

where $\langle \tilde{u}_Y \rangle^+$ is related to $\langle u_Y \rangle^-$ (keeping in mind that $\langle u_Y \rangle^- < 0$) by the rebound law described below. The particle translational velocity after the collision is expressed by means of the impulsive equations and Coulomb's laws. Besides the coefficient of restitution e, the rebound law is expressed by means of the friction factor m. In the case where sliding occurs in the longitudinal direction, and under the condition of negligible spanwise component of the impact velocity for all particles, the mechanical rebound laws for the translational velocity components are:

$$\begin{cases} \tilde{u}_X = u_X + m(1+e)u_Y \\ \tilde{u}_Y = -e\,u_Y \\ \tilde{u}_Z = 0 \end{cases} \Rightarrow \tilde{\mathbf{u}} = \mathbf{C}\,\mathbf{u}\,,\ \mathbf{C} = \begin{bmatrix} 1 & m(1+e) & 0 \\ 0 & -e & 0 \\ 0 & 0 & 0 \end{bmatrix} \tag{5}$$

Such relations are always valid in the incident plane formed by the incident velocity and the wall normal vectors. The reflected velocity lies in this plane too. In this plane, the relation (Eq. (4)) becomes (knowing that $\langle \tilde{u}_Y \rangle^+ = -e\langle u_Y \rangle^-$):

$$x = \frac{e}{1+e} \quad . \tag{6}$$

Note that this value of the parameter x is same as the one obtained in a smooth case since the formalism used by Sakiz and Simonin [9] is based on the following relation:

$$\langle y\,(\mathbf{u})\rangle = \frac{e}{1+e}\langle y\,(\mathbf{u})\rangle^- + \frac{1}{1+e}\langle y\,(\tilde{\mathbf{u}})\rangle^- \tag{7}$$

In opposite to us, they can express $\langle y\,(\tilde{\mathbf{u}})\rangle^+$ as a function of $\langle y\,(\tilde{\mathbf{u}})\rangle^-$ since the rebounds are purely deterministic. By means of Eq. (5) and (7) and making an assumption about the distribution of the wall normal incident particle velocity, Sakiz and Simonin [9] obtained the following boundary conditions at the wall for all computational variables:

$$\left.\begin{aligned} &\langle u_Y \rangle = 0 \\ &\langle u'_X u'_Y \rangle = -m \langle u'^2_Y \rangle \\ &\langle u'^2_X u'_Y \rangle = -2m \langle u'_X u'^2_Y \rangle - m^2 \langle u'^3_Y \rangle \\ &\langle u'^3_Y \rangle = C \frac{1-e}{\sqrt{e}} \langle u'^2_Y \rangle^{3/2} \end{aligned}\right\} \tag{8}$$

where C depends on the distribution of u_Y (in a Gaussian case, $C = -\frac{4}{\sqrt{2p}}$). By analogy with Eq. (8), a model is proposed for the particulate phase boundary conditions in the rough wall case, based on the equivalent Coulomb coefficients e^* and m^*:

$$\left.\begin{aligned} &\langle u'^2_X u'_Y \rangle = -2m^* \langle u'_X u'^2_Y \rangle - m^{*2} \langle u'^3_Y \rangle \\ &\langle u'^3_Y \rangle = C \frac{1-e^*}{\sqrt{e^*}} \langle u'^2_Y \rangle^{3/2} \end{aligned}\right\} \tag{9}$$

where

$$e^* = -\frac{\langle \tilde{u}_Y \rangle^+}{\langle u_Y \rangle^-} \text{ and } m^* = -\frac{\langle u'_X\, u'_Y \rangle}{\langle u'^2_Y \rangle} \tag{10}$$

Note that the zero particle mass flux at the wall is always ensured ($\langle u_Y \rangle = 0$) since the parameter x is defined by $x = \frac{e^*}{1+e^*}$ (similar to Eq. (6)). In the rough wall case, we then rewrite Eq. (3) in the following form, where the effects of the restitution coefficient, friction factor and roughness upon the particle phase boundary conditions at the wall are introduced *via* e^*:

$$\langle y \rangle = \frac{e^*}{1+e^*}\langle y \rangle^- + \frac{1}{1+e^*}\langle y \rangle^+ \tag{11}$$

2.2 Introduction of the 3-D roughness effect

The effect of wall roughness can be introduced into the Eq. (8) by means of the so-called "virtual wall" model of Sommerfeld [2]. In this model, the actual wall is replaced by a virtual wall, whose inclination angle b obeys a centered Gaussian distribution function with a given standard deviation s_b and a zero mean value. The generation of only one inclination angle traduces a 2-D roughness case. In order to extend it to a 3-D case, Sommerfeld & Zivkovic [11] have proposed a rotation of the virtual wall previously generated around the wall normal vector of the real wall. The second inclination angle a obeys a uniform distribution function (in the range $[-p,+p]$). In order to facilitate the calculus, the rotation by a around *Y*-axis is first carried out and then the second rotation by b around z'-axis is applied as it can seen in Fig. 1. We have carried out successively three rotations following the scheme:

$$R(X,Y,Z) \xrightarrow{a} R(x',y',z') \xrightarrow{b} R(x'',y'',z'') \xrightarrow{g} R(x,y,z) \quad (12)$$

The last rotation by g around y"-axis permits to define an incident plane, this will be explained hereafter. The velocity components in the virtual wall co-ordinates system are:

$$\mathbf{u}_{|x'',y'',z''} = \mathbf{P}\,\mathbf{u}_{|X,Y,Z}\,,\ \mathbf{P} = \begin{bmatrix} \cos a\cos b & \sin b & \cos b\sin a \\ -\sin b\cos a & \cos b & -\sin b\sin a \\ -\sin a & 0 & \cos a \end{bmatrix} \quad (13)$$

In order to apply the Coulomb's laws, an incident plane containing the incident velocity vector has to be defined. A new inclination angle g around y"-axis is then defined such as $u_z = 0$:

$$\begin{cases} \cos g = \dfrac{u_{x''}}{\sqrt{{u_{x''}}^2 + {u_{z''}}^2}} \\ \sin g = \dfrac{u_{z''}}{\sqrt{{u_{x''}}^2 + {u_{z''}}^2}} \end{cases} \quad (14)$$

The rotation matrix which permits to obtain the velocity components in the incident plane, noted $\mathbf{I}$, is:

$$\mathbf{u}_{|x,y,z} = \mathbf{I}\,\mathbf{u}_{|x'',y'',z''}\ ,\ \mathbf{I} = \begin{bmatrix} \cos g & 0 & \sin g \\ 0 & 1 & 0 \\ -\sin g & 0 & \cos g \end{bmatrix} \quad (15)$$

In this co-ordinates system, Coulomb's laws can be applied: $\tilde{\mathbf{u}}_{|x,y,z} = \mathbf{C}\,\mathbf{u}_{|x,y,z}$. According to Eq.(5), Eq. (13) and Eq. (15) the post-collisional velocity components with respect to the fixed co-ordinates *X*, *Y* and *Z* become:

$$\tilde{\mathbf{u}}_{|X,Y,Z} = \mathbf{P}^{-1}\mathbf{I}^{-1}\mathbf{C}\,\mathbf{I}\,\mathbf{P}\,\mathbf{u}_{|X,Y,Z} \quad (16)$$

Attention must be paid to the validity of such rebound laws. Sommerfeld and Zivkovic [11], Schade and Hadrich [12] and Sommerfeld and Huber [3] have shown that the distribution of the inclination angle depends on the impact angle of the particle with respect to the wall (the so-called shadow effect). In order to simulate a physical rebound, some values of the virtual wall inclination angle b must be avoided, because the incident and the reflected velocities must satisfy $u_{y''} < 0$ and $\tilde{u}_Y > 0$, respectively. Thus, testing the signs of $\mathbf{u}\cdot\mathbf{n}'$ and $\tilde{\mathbf{u}}\cdot\mathbf{n}$ (where $\mathbf{n}$ and $\mathbf{n}'$ are the unit vectors normal to the actual wall and virtual wall respectively) allows to take the shadow effect into account by disregarding the unphysical cases in the numerical simulation.

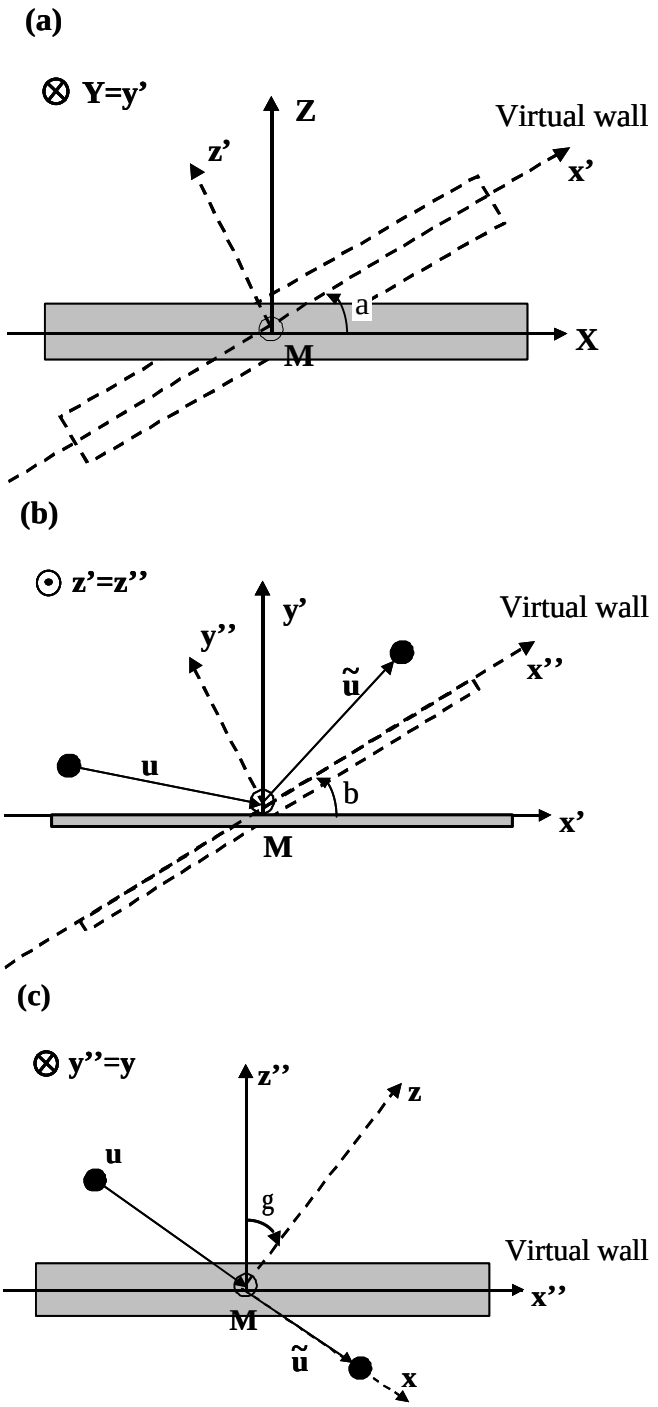

Fig. 1: The 3-D virtual wall model. (a): rotation around Y-axis. (b): rotation around z'-axis. (c) rotation defining an incident plane.

Therefore, taking the shadow effect into account seems of primary importance in order to simulate realistic rebounds. However, up to now, the only work about the Eulerian modelling of the dispersed phase boundary conditions with wall roughness does not take this effect into consideration. This work is by Zhang and Zhou [10], who focused on the dispersed phase boundary conditions, but did not mention any

test on unphysical impacts and reflected angle values, assuming that the inclination of the wall is so small that they can neglect the shadow effect.

3 NUMERICAL SIMULATION, RESULTS AND DISCUSSION

The main objective here is to numerically investigate the dependence of the equivalent coefficients e^* and m^* on the primary collision parameters, mainly the roughness parameter, for a Gaussian distribution of the incident velocity, and to examine the suitability of the proposed model. For this reason, the numerical results about the dispersed phase boundary conditions at the wall are presented with comparison to the results issuing from the model (Eq. (9)). The collisions were assumed to be three-dimensional, *i.e.* the spanwise velocity of the particle was taken into account ($\langle u_Z \rangle^- = 0; \langle u_Z'^2 \rangle^- = 0.2$). For each specification of the collision parameters, we simulated a large number of particle rebounds (10^6) by means of the rebound laws (Eq. (16)). The distribution of the virtual wall inclination angle was Gaussian with given standard deviation s_b and zero mean value. The values of s_b tested here were varied from 0 to 0.2 according to the results of Sommerfeld and Huber [3], who showed that the optimum value of s_b decreases with increasing particle diameter for a given physical roughness. The choice of the value of s_b in practical problems can be made according to the recent work by Sommerfeld [13], who provided correlations of s_b as a function of the particle diameter ($0 < d_p < 500$ µm) for spherical particles. At the present time however, it is not clear how to decide the value of s_b in order to apply such an irregular bouncing model for non spherical particles, although the results obtained by Sommerfeld [14] by means of the exact impulse equations for various particle shapes are very promising in order to develop such a model. The Gaussian distribution of the incident velocity components was prescribed as follows: the tangential and the spanwise incident particle velocities were assumed to obey a Gaussian distribution. In order to close up practical problems, where usually the anisotropic character of the particle velocity variance is observed, therefore the effect of the variation of the ratio $\langle u_X'^2 \rangle^- / \langle u_Y'^2 \rangle^-$ has to be examined here. We present two kinds of results. The first one represents the isotropic case where $\langle u_X'^2 \rangle^- / \langle u_Y'^2 \rangle^- = 1$ and the second one is dedicated to the anisotropic case where the ratio $\langle u_X'^2 \rangle^- / \langle u_Y'^2 \rangle^-$ is equal to 1.5. Whatever the case studied, the following values concerning the spanwise particle velocity and its variance have been imposed. The assumption, lying on the independence of the rotational and translation motion of the particles, is then respected, characterized by: $\langle u_Z'^2 \rangle^- << \langle u_Y'^2 \rangle^-, \langle u_X'^2 \rangle^-$. Calculations were performed for one value of the mean tangential incident velocity, namely $\langle u_X \rangle^- = 10\sqrt{\langle u_Y'^2 \rangle^-}$.

3.1 Study of the equivalent restitution and friction coefficients

Figure 2 illustrates the ratio e^*/e versus the standard deviation of the virtual wall inclination angle s_b. Whatever the value of the ratio $\langle u_X'^2 \rangle^- / \langle u_Y'^2 \rangle^-$, the results are identical. According to the model (Eq. (10)), e^*/e depends only on the distribution function *f* of the incident velocity of the particles at the wall. Whatever the case treated, the Gaussian distribution is used and the wall normal particle velocity variance is the same $\langle u_Y'^2 \rangle^- = 1$, therefore such result is not surprising. In the plot, the ratio e^*/e is seen to increase with increasing s_b. The slope of the curves increases as the restitution coefficient e decreases. As can be observed, e^* is always higher than e. Contrary to e, whose maximum value is equal to unity, e^* can reach considerably higher values. This means that the reflected wall normal velocity can significantly exceed the particle impact velocity as soon as the roughness is present, since $\langle \tilde{u}_Y \rangle^+ = -e^* \langle u_Y \rangle^-$ (with $\langle u_Y \rangle^- < 0$). Accordingly, the wall normal velocity after collision increases as s_b increases. Such a momentum re-distribution due to collisions with a rough wall was noticed in earlier works where gas-solid flows were simulated by Lagrangian particle tracking, like the investigations by Fukagata *et al.* [15] or Sommerfeld [13,16]. As can be observed, the ratio e^*/e is only slightly influenced by the friction coefficient.

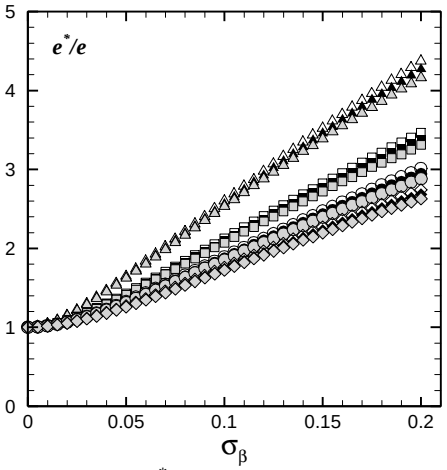

Fig. 2: The ratio e^*/e as a function of the roughness parameter s_b for $\langle u_X'^2 \rangle^- / \langle u_Y'^2 \rangle^- = 1$. e = 0.4: △; e = 0.6: □; e = 0.8: ○; e = 1: ◇. Symbols empty, fill in black and in grey correspond respectively to m = 0.2, 0.3, 0.4.

The evolution of m^*/m as a function of the roughness parameter s_b is displayed in Fig. 3(a)-(b). Comparison of theses figures shows that m^*/m is more affected by the anisotropic character of the particle velocity variance (influence of the value of $\langle u_X'^2 \rangle^-$) than the ratio e^*/e. A non

monotonic behavior of m^*/m is observed, which is more pronounced in the anisotropic case.

The ratio m^*/m first decreases with increasing s_b, and then it increases. In the isotropic case, the influence of e dominates in the first part of the curves, in opposite to the second part where the influence of m is clearly prevailing (the slope change occurs around $s_b \approx 0.05$ whatever the values of the friction and restitution coefficients).

Such observation is less emphasized in the anisotropic case where the influence of e and m seems to be the same in all parts of the curve. In order to study the influence of the shadow effect on these results, $\langle b \rangle$ is plotted as a function of s_b for various values of the restitution and friction coefficients as shown in Fig. 4. Before to describe the obtained results, let us pay attention to what has been done to reveal the shadow effect in a 3-D roughness case. As recommended by Sommerfeld and Zivkovic [11], a has to obey a uniform distribution function in the range $[-p, +p]$.We have observed for such distribution that the shadow effect is not revealed (although it exists) since $\langle b \rangle$ is equal to zero. This result is logical since an inclination angle a generated respectively in the range $\left[-\frac{p}{2}, +\frac{p}{2}\right]$ and $\left[\frac{p}{2}, \frac{3p}{2}\right]$ gives $\langle b \rangle < 0$ and $\langle b \rangle > 0$. Therefore, the result $\langle b \rangle = 0$ is not surprising in the range $[-p, +p]$. Note that the Fig. 4 is related to the case $\left[-\frac{p}{2}, +\frac{p}{2}\right]$. Fortunately, except for the mean value of b, the obtained results are independent of the range chosen for a. We have also observed that the value of $\langle b \rangle$ is the same in the anisotropic and isotropic cases. A unique curve is obtained. Nevertheless, it is interesting to note that the shadow effect is more sensible to the value of the restitution coefficient than the value of the friction coefficient m as it can be seen in Fig. 4. It does not depend on m and decreases slightly with increasing e. Therefore, in that sense, the second part of the curves in Fig. 3(a) seems to be almost independent of the shadow effect since the influence of m was seen to prevail, contrary to the first part of the curves, for which a small value of e corresponds to a maximum influence of the shadow effect. The shadow effect plays exactly the same role in Fig. 3(b) since it is independent of the value of $\langle u_X'^2 \rangle^- / \langle u_Y'^2 \rangle^-$. Figure 3(b) brings the anisotropic effect to light since in this case, the influence of m is clearly noted whatever the value of s_b. Moreover, one can notice that the anisotropy to reduce the value of m^*/m.

Other tests have been carried out showing that a similar behavior is obtained for a value of $\langle u_X'^2 \rangle^- / \langle u_Y'^2 \rangle^-$ equals to 2. In this case, this tendency is more accentuated. This analysis shows that the equivalent parameters e^* and m^* take into consideration the effects related to the roughness of the wall.

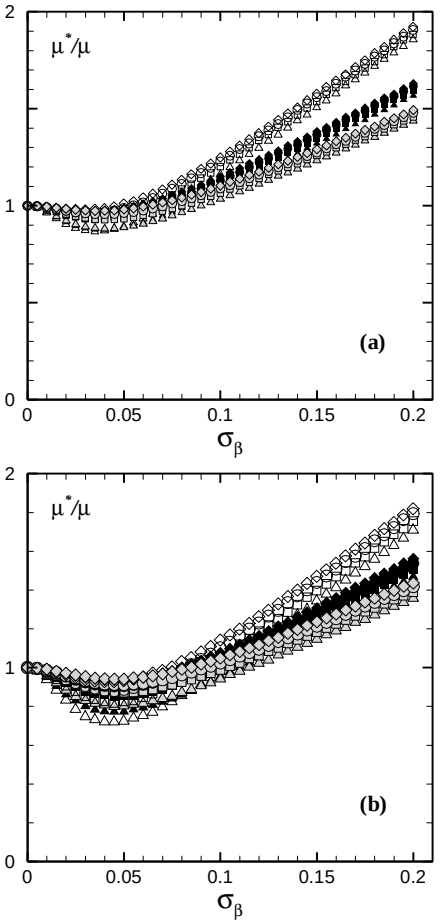

Fig. 3: The ratio m^*/m as a function of the roughness parameter s_b. (a): $\langle u_X'^2 \rangle^- / \langle u_Y'^2 \rangle^- = 1$. (b): $\langle u_X'^2 \rangle^- / \langle u_Y'^2 \rangle^- = 1.5$. Same caption as in Fig. 2.

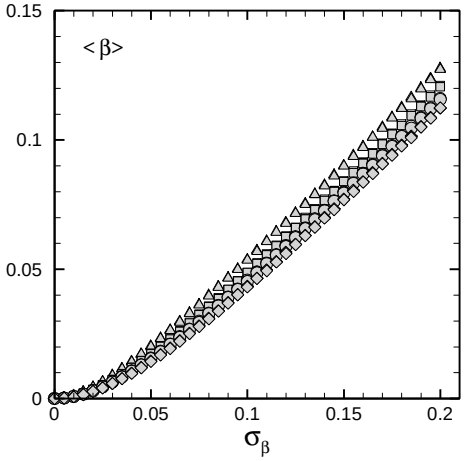

Fig. 4: Influence of the Coulomb parameters on the shadow effect. Same caption as in Fig 2.

Such parameters reproduce, on the one hand, the momentum re-distribution of the particle velocity characterized by e^*, which is increasingly large as s_b is high, and, on the other hand, the antagonistic effects of m^*, *i.e.* a decrease in the equivalent friction for small values of s_b (since for such values the momentum re-distribution is not yet important) and an increase in m^* for larger values of s_b for which the transverse agitation is important. A rapid comparison between these results and those obtained in a two dimensional case permits to observe the effect of the 3-D

character of the roughness. In the whole, all results are more attenuated which is physically correct.

3.2 Evaluation of the proposed model

In order to examine the pertinence of the proposed model, the results issuing from the model and from the numerical simulation are compared in Fig. 5-6, in what concerns the normalized third-order velocity correlations defined by

$$\Pi_{YYY} = \frac{\left\langle u_Y'^3 \right\rangle}{\left\langle u_Y'^2 \right\rangle^{3/2}} \ , \qquad (17)$$

shown in Fig. 5(a)-(b), which should be equal to $C\frac{1-e^*}{\sqrt{e^*}}$ according to the model (Eq. (9)), and

$$\Pi_{XXY} = \frac{\left\langle u_X'^2 u_Y' \right\rangle}{\left\langle u_Y'^2 \right\rangle^{3/2}} \ , \qquad (18)$$

shown in Fig. 6 (a)-(b), which should be equal to $\left[-2m^* \left\langle u_X' u_Y'^2 \right\rangle - m^{*2} \left\langle u_Y'^3 \right\rangle\right] / \left\langle u_Y'^2 \right\rangle^{3/2}$ according Eq. (9).

As it can be seen in Fig 5(a) and 5(b) the obtained values are qualitatively in good agreement with the simulations. The model allows to get a satisfactory estimation of Π_{YYY} whatever the value of $\left\langle u_X'^2 \right\rangle^- \Big/ \left\langle u_Y'^2 \right\rangle^-$. The correlation Π_{XXY} is slightly underestimated by the model for high values of s_b, nevertheless the results are very satisfactory (Fig. 6(a) and 6(b)).

To summarize, acceptable estimates of the velocity correlations at the wall are obtained by means of a formulation close to the smooth wall formulation of Sakiz and Simonin [9], using equivalent restitution and friction coefficients, whose values can be prescribed with the help of Fig. 2 and 3.

4 CONCLUSIONS

In order to obtain the boundary conditions needed in two-fluid models for the dispersed phase in case of irregular particle-wall bouncing, a numerical simulation was carried out by computing the particle statistics at the wall, handling the collisions by means of a 3-D virtual wall model and taking the so-called shadow effect into account. The computational results were analyzed by defining equivalent restitution and friction coefficients (e^*, m^*) which may be used to replace the original coefficients in the available boundary conditions for smooth wall. The obtained results show that the wall roughness has a considerable influence on the equivalent coefficients. Thanks to these new coefficients, a model for the particulate phase boundary conditions is proposed ensuring zero mass flux at the wall. The proposed model leads to good agreement with the results of the numerical simulation. The next step of the study is to investigate the boundary conditions involving the particle rotational velocity components using the same technique, keeping in mind that the existing two-fluid models are still unable to take the rotational motion of the particle into consideration, however.

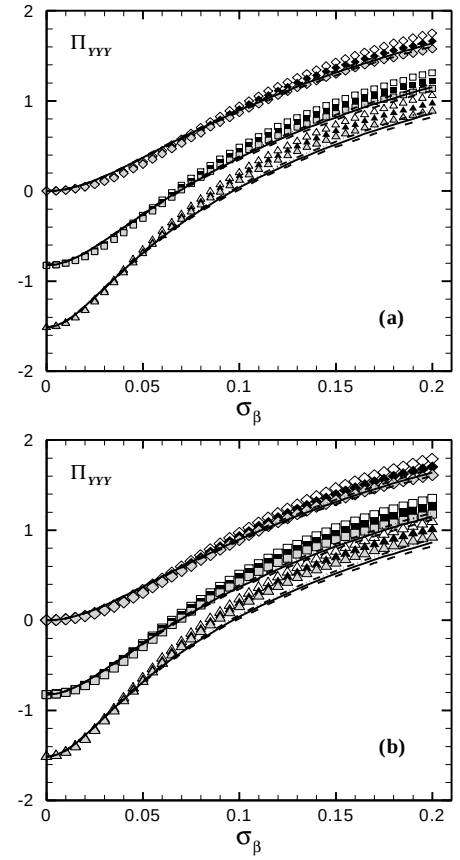

Fig. 5: Comparison between the present model and the numerical results for Π_{YYY}. Same caption as in Fig. 2. Lines: model (Eq.(9)). (a), (b) as in Fig. 3.

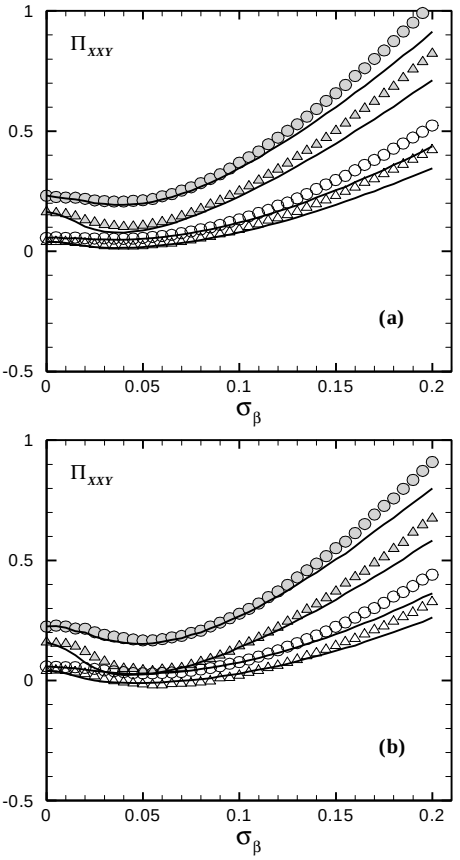

Fig. 6: Comparison between the present model and the numerical results Π_{XXY}. Same caption as in Fig. 2. Lines: model (Eq.(9)). (a), (b) as in Fig. 3.

NOMENCLATURE

e	Normal restitution coefficient for wall-particle interaction (dimensionless)
e^*	equivalent restitution coefficient (dimensionless)
f	Particle velocity distribution function at the wall ($m^{-6}.s^3$)
N	Particle number density at the wall (m^{-3})
N^-, N^+	incident and reflected particle number density at the wall (m^{-3})
$\mathbf{u}$	instantaneous particle velocity vector ($m.s^{-1}$)
$\tilde{\mathbf{u}}$	instantaneous reflected particle velocity vector ($m.s^{-1}$)
u_X, u_Y, u_Z	streamwise, wall-normal and spanwise velocity components ($m.s^{-1}$)
u'_X, u'_Y, u'_Z	fluctuations of velocity components ($m.s^{-1}$)

Greek letters

a, b	inclination angles of the virtual wall (radian)
g	inclination angle defining an incident plane (radian)
s_b	standard deviation of the inclination angle of the virtual wall (radian)
m	Friction coefficient for wall-particle interaction (dimensionless)
m^*	equivalent friction coefficient (dimensionless)

Subcripts

x, y, z	direction of vector components in orthogonal system $R(x, y, z)$
x', y', z'	direction of vector components in orthogonal system $R(x', y', z')$
x'', y'', z''	direction of vector components in orthogonal system $R(x'', y'', z'')$

Others

$\langle . \rangle$	global average
$\langle . \rangle^-$, $\langle . \rangle^+$	average on respectively incident and reflected particles

REFERENCES

1. Y. Tsuji, Y. Morikawa, T. Tanaka, N. Nakatsukasa, M. Nakatami, Numerical simulation of gas-solid two phase flow in a two dimensional horizontal channel, *Int. J. Multiphase Flow*, vol. 13, pp. 671-684, 1987.
2. M. Sommerfeld, Modelling of particle/wall collisions in confined gas-particle flows, *Int. J. Multiphase Flow*, vol. 18, pp. 905-926, 1992.
3. M. Sommerfeld and N. Huber, Experimental analysis and modelling of particle-wall collisions, *Int. J. Multiphase Flow*, vol. 25, pp. 1457-1489, 1999.
4. I.V. Derevich, L.I. Zaichik, Particle deposition from turbulent flow, *Fluid Dynamics*, Vol. 23, pp. 722-729, 1988
5. D.C. Swailes, M.W. Reeks, Particle deposition from a turbulent flow. I. A steady-state model for High inertial particles. *Phys. Fluids*, Vol. 6 (10), pp. 3392-3403, 1994.
6. B.J. Devenish, D.C. Swailes, Y.A. Sergeev, V.N. Kurdyumov, A PDF model for dispersed particles with inelastic particle-wall collisions, *Phys. Fluids*, Vol. 11(7), pp.1858-1868, 1999.
7. V.M. Alipchenkov, L.I. Zaichik, O. Simonin, A comparison of two approaches to derivation of boundary conditiond for continuous equations of particle motion in turbulent flow, *High Temp.*, Vol. 39(1), pp. 104-110, 2001.
8. J. He, O. Simonin, Non-equilibrum predictions of the particle phase stress tensor in vertical pneumatic conveying. In: D. Stock (Ed.), *Proc. 5th Int. Symp. on Gas-Solid Flows*, ASME Fluids Engineering Division Summer Meeting, Washington, D.C., Vol. 166, pp. 253-263, 1993.
9. M. Sakiz and O. Simonin, Development and validation of continuum particle wall boundary conditions using Lagrangian simulation of a vertical gas-solid channel flow, In: *Proc. 3rd ASME/JSME Joint Fluids Eng. Conf.*, San-Francisco, CA, Paper N° 7898, 1999.
10. X. Zhang and L.X. Zhou, A two-fluid particle-wall collision model accounting for the wall roughness. In: M. Sommerfeld (Ed.), *Proc. 10th Workshop on Two-Phase Flow Predictions*, Merseburg, Germany, pp. 44-51, 2002.
11. M. Sommerfeld and G. Zivkovic, Recent advances in the numerical simulation of pneumatic conveying trough pipe systems. In: Hirsch, Ch., Periaux, J., Onate, E. (Eds.), *Computational Methods in Applied Science*. Invited Lectures and Special Technological Sessions of the First European Computational Fluid Dynamics Conference and the First Conference on Numerical Methods in Engineering, Brussels, pp. 201-212, 1992.
12. K.P. Schade and Th. Hadrich, Investigation of influence of wall roughness on particle-wall collisions. In: *Proc. 3rd Int. Conf. on Multiphase Flow*, ICMF'98, Lyon, France, Paper N° 250, 1998.
13. M. Sommerfeld, Analysis of collision effects for turbulent gas-particle flow in a horizontal channel: Part I. Particle transport, *Int. J. Multiphase Flow*, vol. 29, pp. 675-699, 2003.
14. M. Sommerfeld, Kinetic simulations for analysing the wall collision process of non-spherical particles. *In: Proc. ASME Fluids Eng. Division Summer Meeting*, Montreal, Canada, Paper N° 31239, 2002.
15. K. Fukagata, S. Zahrai, F. Bark, S. Kondo, Effects of wall roughness in a gas-particle turbulent vertical channel flow. In: Lingborg et al. (Eds.), *Proc. 2nd Int. Symp. on Turbulence and Shear Flow Phenomena*, KTH, Stockholm, II, pp. 117-122, 2001.
16. M. Sommerfeld, The importance of inter-particle collisions in horizontal gas-solid channel flows. *In: Proc. ASME Fluids Eng. Division Conf.*, vol. 228, Hiltons Head, pp. 335-345, 1995.